This is the final draft post-refereeing.

The publisher's version can be found at https://pubs.acs.org/doi/10.1021/acs.biomac.0c00186

Please cite this article as: Monge-Morera, M. Lambrecht, M.A., Deleu, L.J., Gallardo, R., Louros, N.N., De Vleeschouwer, M., Rousseau, F., Schymkowitz, J. and Delcour, J.A. Processing induced changes in food proteins: amyloid formation during boiling of hen egg white, Biomacromolecules, 2020, xx, xxxx-xxxx, doi: xxxxx.

Processing induced changes in food proteins: amyloid formation during boiling of hen egg white

Margarita Monge-Morera[1], Marlies A. Lambrecht[1], Lomme J. Deleu[1], Rodrigo Gallardo[2,3], Nikolaos N. Louros[2], Matthias De Vleeschouwer[2], Frederic Rousseau[2], Joost Schymkowitz[2*], Jan A. Delcour[1*]*

[1]KU Leuven, Laboratory of Food Chemistry and Biochemistry and Leuven Food Science and Nutrition Research Centre (LFoRCe), Kasteelpark Arenberg 20, B-3001 Leuven, Belgium

[2]KU Leuven, Switch laboratory, Department of Cellular and Molecular Medicine, Herestraat 49, B-3001 Leuven, Belgium

[3]University of Leeds, Astbury Centre for Structural Molecular Biology, School of Molecular and Cellular Biology, Garstang Building, LS2 9JT Leeds, United Kingdom

*Corresponding authors: frederic.rousseau@kuleuven.vib.be (Tel: +3216372572), joost.schymkowitz@kuleuven.vib.be (Tel: +3216372573), jan.delcour@kuleuven.be (Tel: +3216321581)

ABSTRACT

Amyloid fibrils (AFs) are highly ordered protein nanofibers composed of cross β-structure that occur in nature, but that also accumulate in age-related diseases. Amyloid propensity is a generic property of proteins revealed by conditions that destabilise the native state, suggesting that food processing conditions may promote AF formation. This had only been shown for foie gras, but not in common foodstuffs. We here extracted a dense network of fibrillar proteins from commonly consumed boiled hen egg white (EW), using chemical and/or enzymatic treatments. Conversion of EW proteins into AFs during boiling was demonstrated by thioflavin T fluorescence, Congo red staining and X-ray fibre diffraction measurements. Our data show that cooking converts approximately 1-3% of the protein in EW into AFs, suggesting that they are a common component of the human diet.

KEYWORDS: cross β-sheet, food protein aggregation, ovalbumin, enzymatic or chemical extraction, X-ray diffraction pattern

INTRODUCTION

Protein amyloid fibrils (AFs) are self-assembled fibrillar protein aggregates with a cross β-sheet core. The β-strands are stacked perpendicular to the fibril axis and stabilised by hydrogen bonds[1,2]. This structure endows the fibrils with a remarkable chemical resistance and mechanical strength[3], making AFs interesting building blocks for functional protein-based materials[4,5]. AFs occur in nature, for instance, bacteria employ them as a colonization tool, insect larvae in their eggshells, and even in mammalians AFs are functionally employed, for example to regulate melanin synthesis, hormone storage or memory formation[6,7]. Moreover, AF formation is much studied in the context of age-dependent degenerative conditions, including neuronal pathologies such as Alzheimer or Parkinson's and non-neuronal diseases, such as type 2 diabetes or systemic amyloidosis[8]. Despite the fact that only 40 or so amyloid-associated diseases are known, bioinformatics work showed that amyloid propensity is widespread in the proteome and encoded by aggregation prone polypeptide segments[9–11]. The amyloid propensity is inhibited by the native fold of the protein and can be revealed by exposing the protein to conditions that destabilise native state, such as low pH or elevated temperature[8]. Common food-processing methods thus include conditions that have been shown to promote amyloid formation for many proteins[12], including food-borne proteins in purified form[13,14]. However, prior to the present work, the only food in which AFs have indisputably been shown to be present are duck and goose derived foie gras[15].

Heating the commonly consumed hen (*Gallus gallus domesticus*) egg white (EW) induces protein network and gel formation during which intermolecular β-sheet structures are formed[5,16,17]. Ovalbumin (OVA) (*ca*. 54%), ovotransferrin (*ca.* 12%), ovomucoid (*ca.* 11%), ovomucin (*ca.* 4%) and lysozyme (*ca*. 4%) are the most abundant EW proteins[18]. AF formation is studied with isolated OVA, lysozyme and EW as a whole[13]. Desalted solutions of EW powder (73 g/L) form short linear

aggregates of about 20 to 150 nm as a result of heating (78 °C for 22 h at pH 7.0), cooling (to 20°C) and adjusting the pH to 4.5. Their contour length is longer (50-350 nm rather than 20-150 nm) when EW preparations do not contain ovotransferrin[19]. Stretched films of poached EW show X-ray diffraction patterns compatible with cross-β structures[20]. Yet, the level of EW amyloid-like aggregates is lower than obtained with solutions of pure OVA[5]. When heated to between 65 °C to 90 °C at acidic pH[21–26] or to between 40 °C to 80 °C at neutral pH for several hours to days[5,23,27–33] OVA forms amyloid-like protein fibrils. The impact of processing on AF formation from OVA was recently reviewed[13]. Heat-treated OVA [2.0% (w/v), pH 2.0 or 7.0, 60 °C to 80 °C, 60 or 1200 min] amyloid-like aggregates consist of a compact core surrounded by loosely packed protein segments[23,29]. Semi-flexible unbranched fibrils with contour lengths of 400 to 700 nm result from heating 2.0% (w/v) OVA at 78 °C for 22 h at neutral pH and low ionic strength[27]. However, the typical X-ray diffraction pattern of the cross-β motif has not been described for heated OVA amyloid-like aggregates. In spite of the above work, the potential presence of fibrils in boiled eggs which meet all criteria to be classified as AFs remained to be investigated.

We here show that AFs are formed during egg boiling. That EW rapidly gels upon boiling evidently complicates the identification of fibrillary protein structures as most methods require protein to be solubilised/suspended. To overcome this problem, fibrillary structures were extracted from EW gels using chemicals or enzymes. Compact amyloid structures are less susceptible to chemical or enzymatic cleavage than amorphous protein aggregates[14,34–36]. We successfully used proteinase K and subsequent solubilisation with hydrochloric acid solution to extract fibrils from boiled EW. These fibrils were indisputably identified as AFs.

EXPERIMENTAL SECTION

Materials. EW [*ca.* 90% protein on dry matter (dm) basis] was isolated from commercial eggs as commonly done. Dithiothreitol and sodium azide were from Acros Organic (Geel, Belgium). Sodium dodecyl sulfate, sodium dihydrogen phosphate dihydrate, sodium chloride and urea were from VWR International (Leuven, Belgium). Bovine serum albumin standard (23209) was from ThermoFisher Scientific (Waltham, MA, USA). OVA (albumin chicken egg grade III*, ca.* 94% protein on dm basis), proteinase K (*Tritirachium album,* P4850), trypsin (porcine pancreas, T0303) and all chemicals (of at least analytical grade), unless specified otherwise, were from Sigma Aldrich (Bornem, Belgium). Enzyme units (EU) were as specified by the supplier. The highly amylogenic peptide (residues: 103-111) derived from sup35 yeast was produced in-house[37].

Heat treatment of egg white and ovalbumin. Fresh EW (15.0 g) was boiled for 15 min at 100 °C in sealed plastic cans (inner and outer diameters 4.0 cm and 4.3 cm respectively, height = 3.0 cm). The core of the EW gel was cut in small pieces and used in further analysis. An aliquot (1.0 ml) of 5.0% (w/v) OVA was heated in sealed glass tubes (inner and outer diameters 1.2 and 1.5 cm respectively, height = 10 cm) at 78 °C and 100 °C for different times. Also, 2.0 ml 2.0% (w/v) OVA was heated at 78 °C for 22 h ($OVA_{78/22h}$) as described previously[27].

Protein fibril isolation. To unheated and heated samples containing about 32.0 mg of OVA or EW protein was added an amount of SDS and/or DTT containing medium such that a total volume of 1.6 ml was obtained which contained 0.0%, 0.1%, 0.2%, 0.3%, 0.5% or 0.8% (w/v) SDS, 0.02% (w/v) sodium azide and, optionally, 1.0% (w/v) DTT. The samples were shaken at room temperature (RT) (16 h, 150 rpm). The supernatants obtained by centrifugation (9,300 *g*, 15 min, RT) were analysed.

Enzymatic treatment and protein fibril isolation. Aliquots of proteinase K (5.2 µl containing *ca.* 4 EU) or trypsin (13 µl containing *ca.* 3.38 to 5.20 kEU) were added to samples containing *ca.* 32.0 mg (un)heated protein. The samples were then incubated at 37 °C for 48 h under continuous shaking (150 rpm). The supernatant (*i.e.* soluble fraction 1) obtained by centrifugation (9,300 *g*, 15 min, RT) was analysed. Protein fibrils contained in the separated EW pellet produced after proteinase K treatment (*ca*. 75.0 mg) were extracted (RT, 1 h, 150 rpm) by adding aliquots (1.5 ml) of 0.01 M, 0.05 M, or 0.1 M HCl. The supernatants (*i.e.* soluble fraction 2) obtained by centrifugation (9,300 *g*, 15 min, RT) were analysed.

Analysis of protein content. The protein contents of diluted OVA and EW extracts obtained after chemical or enzymatic treatment were determined in triplicate by analysis of ultraviolet (UV) extinction (280 nm). Samples (200 µl) transferred to UV-star plates (Greiner Bio-One, Vilvoorde, Belgium) were analysed in a Synergy Multi-Mode Microplate Reader (BioTek, Winooski, VT, USA). Absorbance values were converted to protein concentrations using a calibration curves constructed with unheated OVA and EW (R^2= 0.9987 and R^2= 0.9974; respectively).

Analysis of thioflavin T fluorescence. Thioflavin T fluorescence is an indication of the level of cross-β sheet structures[38]. In a black 96-well plate (Greiner Bio-One), sample (190 µl) was mixed with 10 µl 200 µM ThT. Triplicate fluorescence measurements were performed in a Synergy Multi-Mode Microplate Reader (BioTek). The excitation and emission wavelengths were 440 nm and 480 nm, respectively. The reference [*i.e.* 2.0% (w/v) $OVA_{78/22h}$] and extracted/isolated protein samples were diluted to the same protein content [0.05 % (w/v) or 0.1% (w/v)] with 0.05 M sodium phosphate buffer (pH 7.0, SPB). This dilution with SPB buffer prevents differences in ThT intensity due to differences in pH or viscosity. The latter can restrict the rotation of the benziothiazole and the aminobenzene rings of the ThT molecule[39,40]. ThT fluorescence is

expressed as the fluorescence intensity of the sample relative to that of the above mentioned sup35 yeast peptide (*i.e.* NFNYNNNLQG) under the applied experimental conditions.

Microscopy of Congo red stained samples. AFs have a typical green birefringence when stained with Congo red. Enzyme treated OVA and EW protein samples were concentrated by centrifugation (10,000 *g* for 15 min) using an Amicon Ultra-0.5 centrifugal filter device 50 K (Merck, Darmstadt, Germany). Aliquots (first 10 µl and 4 to 7 µl for the subsequent additions) of the concentrated samples were dried on a microscope slide repeatedly. After drying, 7 to 10 µl 0.1% (w/v) Congo red was added (RT, 30 min, dark room). Afterwards, samples were washed several times with 90% (w/w) ethanol prior to being studied under bright and polarised light with a SM2 800 optical microscope (Nikon, Tokyo, Japan) equipped with a camera and Nikon NIS-Elements Viewer 4.20 software.

Size exclusion chromatography. The apparent molecular weight (MW) distribution of protein aggregates was evaluated in triplicate using SE-HPLC[41]. Samples (1.0 ml) combined with 43 µl 200 µM ThT were filtered (Millex-HP, 0.45 µm, polyethersulfone; Millipore, Carrigtwohill, Ireland) and loaded on a Biosep-SEC-S3000 (size range 5-700 kDa, 25 µl, 0.5 ml SPB/min) or Biosep-SEC-S4000 (size range 15-1,500 kDa, 23 µl, 1.0 ml SPB/min) (Phenomenex, Torrance, CA, USA) column at 30 °C. SE-HPLC was conducted using a LC-20AT system (Shimadzu, Kyoto, Japan) with automated injection, monitoring 280 nm UV extinction, and using 450 and 480 nm as excitation and emission wavelengths for ThT fluorescence detection.

Multi-angle light scattering. The MW of the protein aggregates was studied using multi-angle light scattering (MALS) on a DAWN HELEOS MALS instrument from Wyatt Technology (Santa Barbara, CA, USA) with an incident laser wavelength of 658 nm. The protein aggregates were separated by SE-HPLC with an LC-10 Prominence system (Shimadzu) using conditions similar as

described above. Duplicate aliquots (25 µL) of a solution containing 2.0 mg protein/ml were injected at RT. The scattering intensities at different angles were collected, corrected for the refractive indices of glass and solvent and normalised using bovine serum albumin. The value of d*n*/d*c* (wherein *n* is the refractive index of the solution and *c* the solute concentration) was set to 0.185 ml/g and the scattering data (collected at an interval of 0.5 seconds) were then fitted according to Zimm formulation, which relates the excess of incident light scattered to the molecular structure[42].

Transmission electron microscopy. The morphology of protein aggregates was studied with TEM. Samples (10 µl) were loaded for 3 min on glow discharged copper grids of 400-mesh which were coated with formvar film (Agar Scientific, Stansted, United Kingdom). After sample adsorption, the excess sample was drained with filter paper. Then, samples were washed with MilliQ water and stained with 2.0% (w/v) uranyl acetate in MilliQ water for 45 s. Stained samples were washed a second time with MilliQ water and drained with filter paper. The grids were dried for 5 min at RT and examined using a JEM-1400 TEM (Jeol, Tokyo, Japan) instrument at 80 keV.

Attenuated total reflection Fourier transform infrared spectroscopy. The secondary structure of samples (35 µl) containing 0.1% (w/v) protein was investigated with attenuated total reflection Fourier transform infrared spectroscopy (ATR-FTIR) in a Bruker (Karlsruhe, Germany) Tensor 27 infrared spectrophotometer equipped with a Bio-ATR II accessory (Harrick Scientific Products, Pleasantville, NY, USA). The instrument was continuously purged with dry air. Spectra were recorded in the 850 to 4,000 cm^{-1} range at a resolution of 2 cm^{-1} by accumulating 256 data acquisitions, corrected for atmospheric water vapor interference, baseline-subtracted, and vector normalised in the Amide I area (1,600 to 1,700 cm^{-1}). Maximum peaks were assigned with peak picking based on the second derivative, as implemented in Bruker OPUS software.

X-ray diffraction measurements. The crystalline structure along the fibre axis was studied with X-ray diffraction. Protein extracts concentrated by centrifugation (10,000 *g* for 15 min) using an Amicon Ultra-0.5 centrifugal filter device (50 K) were dried and the fibres formed between two wax tipped capillary tubes were analysed. X-ray diffraction patterns were collected using a Rigaku (Tokyo, Japan) copper rotating anode (RA-Micro7 HFM) operated at 40 kV and 30 mA and a wavelength l = 1.54 Å. The specimen-to-film distance was 275 mm and the exposure time 900 s. Diffraction patterns were studied using Adxv software (Scripps Research, La Joya, CA, USA) and displayed with iMosFLM[43].

Statistical analysis. Significant differences ($\alpha < 0.05$) based on at least three individual measurements were determined with a one-way ANOVA procedure using JMP® Pro 14.0.0 (SAS Institute, Cary, NC, USA). Corresponding Tukey grouping coefficients are given.

RESULTS AND DISCUSSION

Identification of amyloid fibrils in boiled hen egg white

AFs display the following properties that can hence be used to unequivocally identify this protein structure: a fibrillar morphology as visualized by transmission electron microscopy (TEM), a high level of β-sheet structures as shown by thioflavin T (ThT) fluorescence and Fourier transform infrared (FTIR) spectroscopy, green birefringence upon staining with Congo red and, widely regarded as the strongest evidence, a unique X-ray diffraction pattern with reflections at 4.7 Å (meridional) and 9-12 Å (equatorial), which correspond to the inter β-strand spacing and the distance between stacked β-sheets, respectively[2,44]. Dilute hydrochloric acid (HCl) (0.01 M, 0.05 M or 0.10 M) extracted almost all fibrillary EW structures in pellets obtained after proteinase K treatment of 15 min boiled EW ($EW_{100/15min}$) resulting in ThT fluorescence values in the extracts

of *ca*. 20% compared with the intensity of a sample of mature AFs of yeast prion sup35 peptide (residues: 103-111) at the same protein concentration in monomeric units. FTIR spectra of the 0.01 M HCl extract confirmed the presence of β-sheet structures (Figure 1.a). In addition, TEM images indicated the presence of worm-like protein fibrils of variable sizes (Figure 1.e, Figure 1.f and Figure S1). The extracted protein also showed the characteristic amyloid green birefringence after staining with Congo red (Figure 1.c and Figure 1.d). Its X-ray diffraction pattern showed typical amyloid reflections at 4.7 Å and 10.2 Å confirming that AFs are formed during EW boiling. An estimated 1.5-3.0% of EW proteins assemble into AFs during boiling [calculated by comparing the amount of protein of the size-exclusion high performance liquid chromatography (SE-HPLC) peak A of the boiled EW tryptic digest with a high ThT fluorescence (Figure 3.e) and the initial protein content].

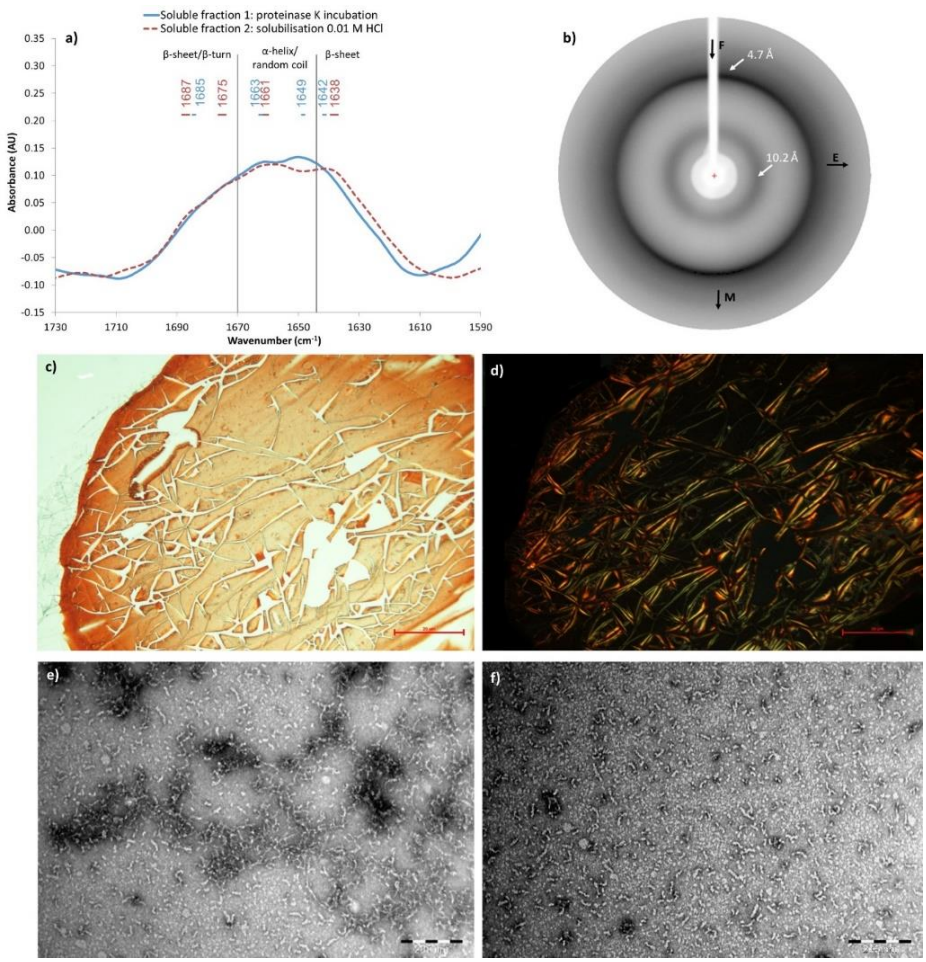
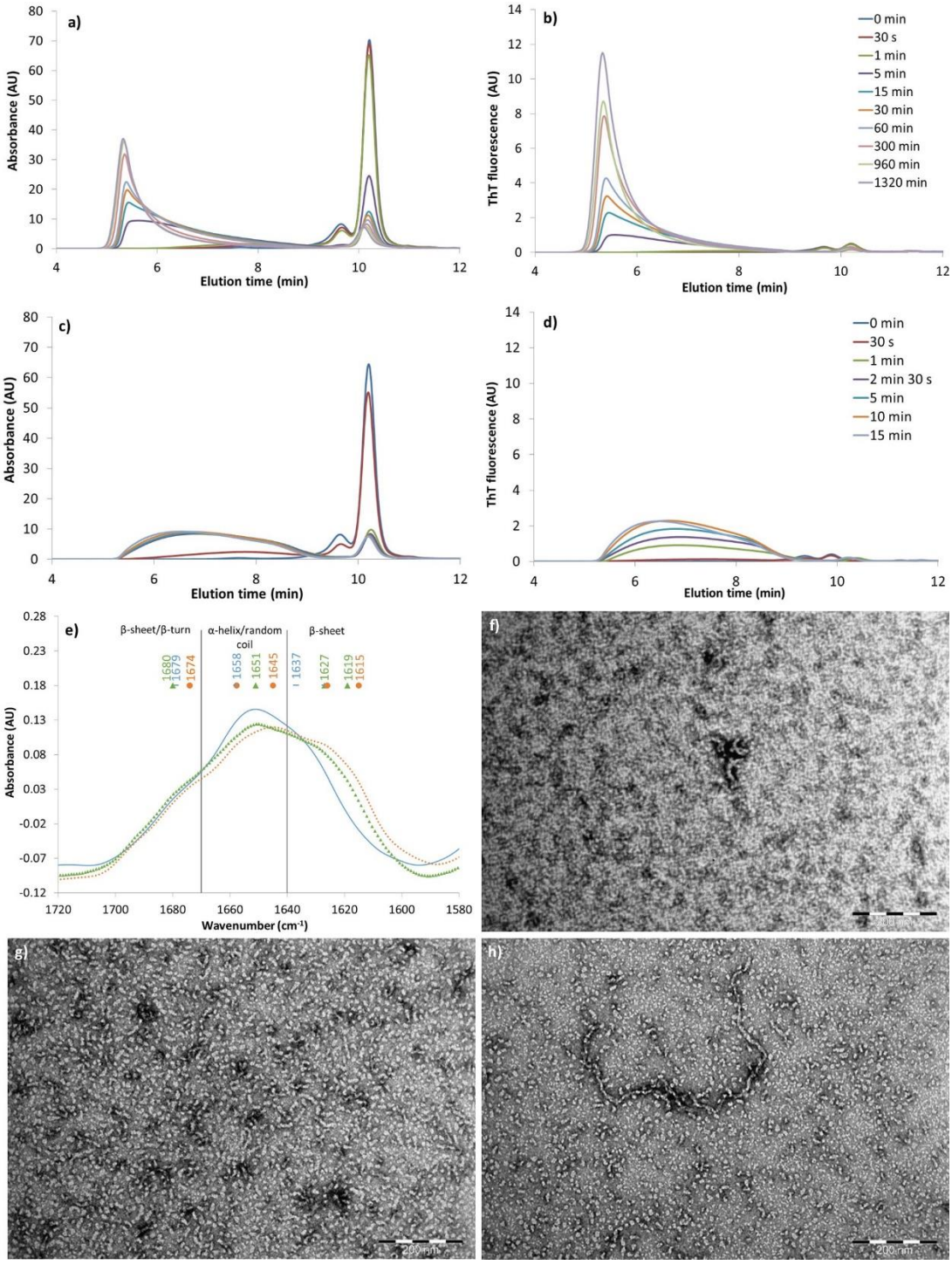


Figure 1. Amyloid fibrils (AFs) in egg white (EW) boiled for 15 min ($EW_{100/15min}$). FTIR spectrum (a) of soluble fraction 1 (proteinase K incubation of $EW_{100/15min}$) and of soluble fraction 2 (solubilisation with 0.01 M HCl of the pellet produced after proteinase K treatment of $EW_{100/15min}$). Wavenumbers in (a) are detected with the peak picking tool based on the second derivative. Vertical lines in (a) separate the wavenumbers assigned to the secondary structure of proteins. AU, arbitrary units. X-ray diffraction pattern (b) of soluble fraction 2. Congo red stained sample of pellet obtained from $EW_{100/15min}$ pellet after proteinase K treatment observed under bright light (c) and under cross-polar light (d). Scale bar: 20 µm. Transmission electron microscopy (TEM) images (e and f; scale bar: 200 nm) of the soluble fraction 2.

Enzymatic digestion for isolating protein fibrils

To exclude the impact of the extraction procedure on the formation of EW AFs, we tested the above described proteinase K treatment also on OVA fibrils. OVA heated at 78 °C for 22 h ($OVA_{78/22h}$) was included as positive control as it contained larger worm-like fibrils (Figure 2.a) than OVA boiled for 15 min ($OVA_{100/15min}$) (Figure 2.c). Indeed, while TEM images of $OVA_{100/15min}$ (Figure 2.h and Figure S2) showed (clusters of) short worm-like fibrils with an average length of maximally *ca.* 80 nm, $OVA_{78/22h}$ (Figure 2.g and Figure S2) showed predominantly short (< *ca.* 120 nm) but also longer (> *ca.* 200 nm) worm-like fibrillary protein complexes. In addition, fluorescence density, *i.e.* the area of ThT fluorescence relative to that of UV absorbance, measurements showed higher levels of β-sheet structures in $OVA_{78/22h}$ than in $OVA_{100/15min}$. In both samples, the maximum wavenumbers of the second derivative in the FTIR spectrum indicated the presence of β-sheet structures (Figure 2.e). Noteworthy, non-aggregated proteins and some large worm-like protein aggregates with a length of *ca.* 200 nm were detected with TEM in native OVA (Figure 2.f and Figure S2).

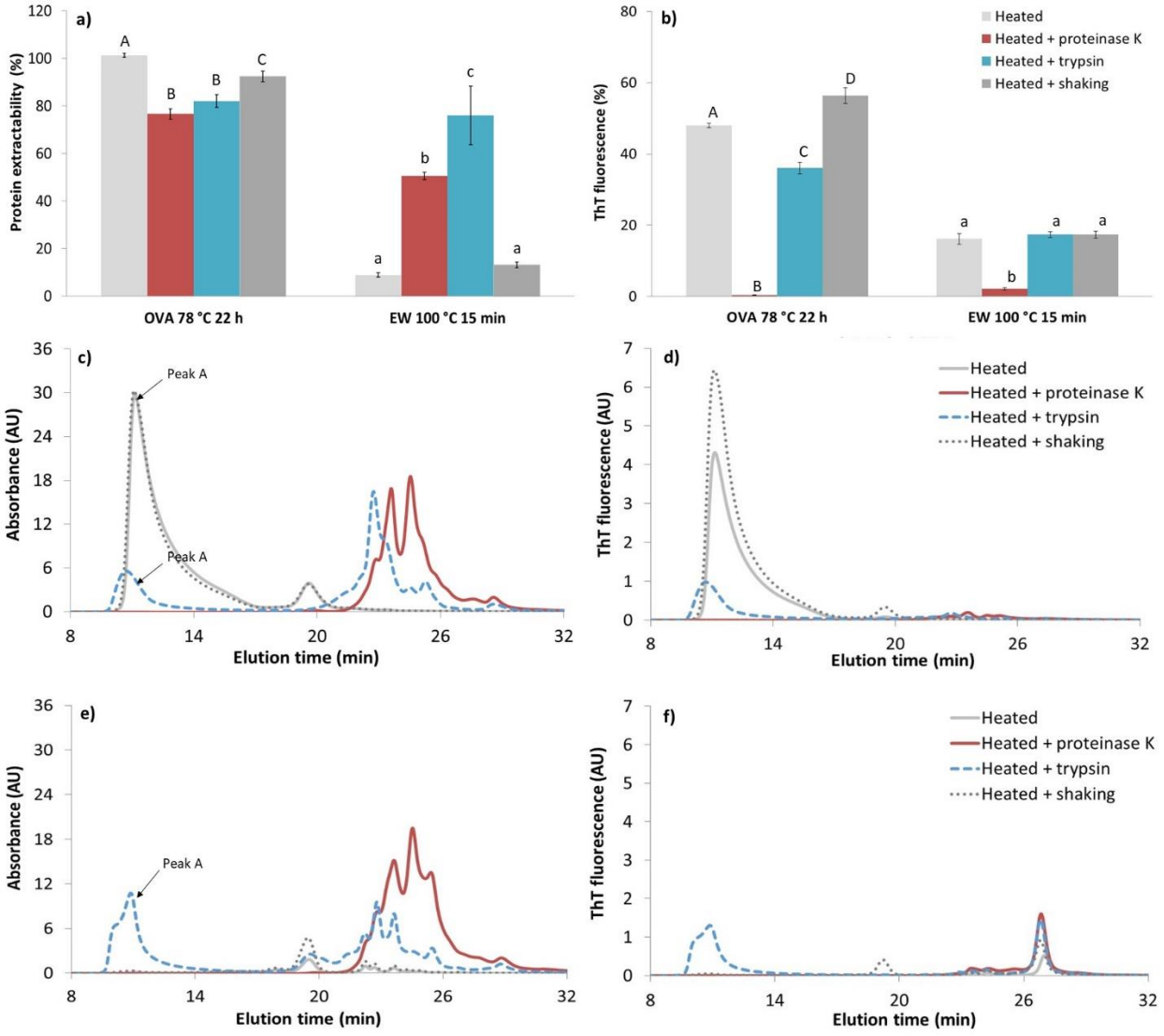


232

233 Figure 2. Impact of heating on ovalbumin (OVA) protein fibrillation. SE-HPLC profiles of
234 ovalbumin (OVA) heated at 78 °C (a, b, OVA78) and 100 °C (c, d, OVA100) for various times.
235 OVA showed peaks at ca. 9 min and 55 s and 10 min and 22 s which correspond to OVA dimers

(*ca.* 76 kDa) and monomers (*ca.* 40 kDa), respectively. UV absorbance (a, c) and thioflavin T (ThT) fluorescence (b, d) were measured. FTIR spectrum (e) and transmission electron microscopy (TEM) images (scale bar: 200 nm) of unheated (— in e, f) and heated ovalbumin (OVA) for 22 h at 78 °C (····· in e, g, $OVA_{78/22h}$) and OVA heated for 15 min at 100 °C (▲ in e, h, $OVA_{100/15min}$). Wavenumbers shown in (e) were detected with the peak picking tool based on the second derivative. Vertical lines in (e) separate the wavenumbers assigned to the secondary structure of proteins. AU, arbitrary units.

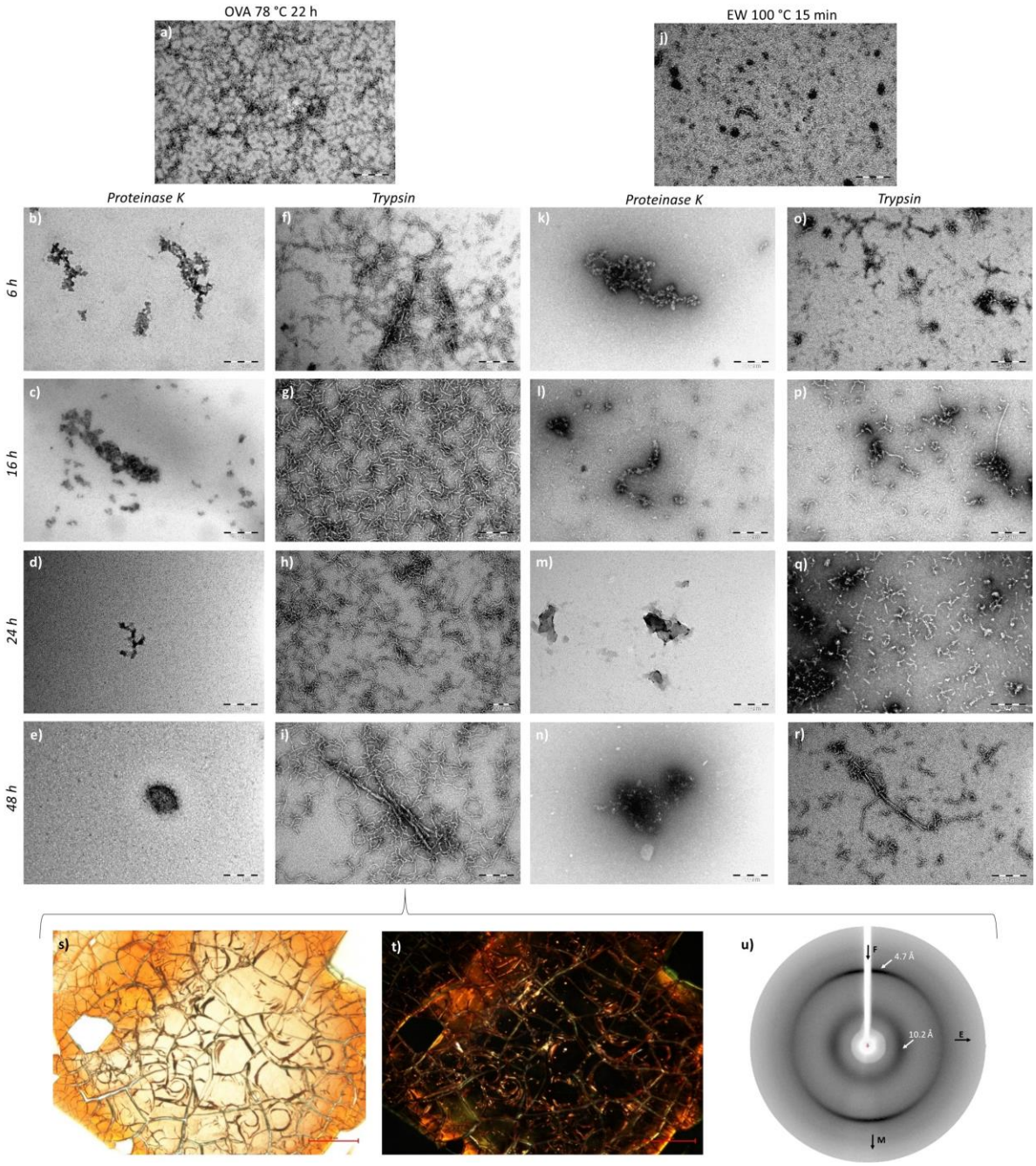
The supernatants obtained after 6 and 48 h proteinase K treatments of $OVA_{78/22h}$ and $EW_{100/15min}$ and centrifugation (Figure 3.a and Figure S3) had ThT fluorescence readings which were drastically lower than those of control samples which had undergone the same treatments but without proteinase K addition (Figure 3.b and Figure S3). More in particular, SE-HPLC profiles of $OVA_{78/22h}$ and $EW_{100/15min}$ extracts revealed no or only a slight enhancement in ThT fluorescence as a result of proteinase K treatment (Figure 3.c and Figure 3.d, Figure 3.e and Figure 3.f, respectively). In addition, TEM images of $OVA_{78/22h}$ and $EW_{100/15min}$ extracts obtained with 6 h proteinase K treatment showed mainly amorphous protein aggregates (Figure 4 and Figure S4). The above allowed speculating that the pellet recovered by centrifugation following proteinase K treatment of $OVA_{78/22h}$ and $EW_{100/15min}$ contained AFs.



253

254 Figure 3. Impact of peptidase treatment on protein fibril extractability derived from heated
255 ovalbumin ($OVA_{78/22h}$) and egg white boiled for 15 min ($EW_{100/15min}$). Protein extractability (a)
256 and thioflavin T (ThT) fluorescence (b) of $OVA_{78/22h}$ and $EW_{100/15min}$ treated with proteinase K or
257 trypsin. Shaking (150 rpm) was for 48 hours at 37 °C. Results with the same letters are not
258 significantly different in $OVA_{78/22h}$ (uppercase) and $EW_{100/15min}$ (lowercase) [$P < 0.05$]. SE-HPLC
259 UV profiles of $OVA_{78/22h}$ (c, d) and $EW_{100/15min}$ (e, f) treated with proteinase K or trypsin. UV
260 absorbance (c, e) and thioflavin T (ThT) fluorescence (d, f) were measured. AU, arbitrary units.

In addition, an alternative method based on proteolytic degradation of the sample with trypsin was developed. As trypsin preferentially cleaves after lysine and arginine residues and these charged amino acids are generally not present in aggregation prone sequences leading to AFs, it was also used in the present work to treat $EW_{100/15min}$ or solutions of $OVA_{78/22h}$. When shaking $OVA_{78/22h}$ and $EW_{100/15min}$ samples with trypsin, the isolation yield/extractability of protein from both samples was about 80% (Figure 3.a). The ThT fluorescence of these samples was significantly lower (for $OVA_{78/22h}$) or similar (for $EW_{100/15min}$) to that of those which also had been shaken, but without enzyme (Figure 3.b). Trypsin treatment (6 h) caused a slight decrease in the ThT fluorescence of the $OVA_{78/22h}$ extract to a plateau value of *ca*. 36% (Figure S3). In contrast, the ThT fluorescence of $EW_{100/15min}$ (*ca.* 20%) was not impacted by the enzymatic treatment (Figure S3). SE-HPLC profiles of $OVA_{78/22h}$ and $EW_{100/15min}$ samples treated with trypsin showed large protein (peak A) aggregates (elution time *ca*. 10 – 12 min; *ca*. 15,000 k and 24,000 k respectively) with enhanced ThT fluorescence (Figure 3.c and Figure 3.d, Figure 3.e and Figure 3.f, respectively). In addition, large (> 200 nm) worm-like fibrillary aggregates were observed when peak A material of $OVA_{78/22h}$ and $EW_{100/15min}$ was subjected to TEM (Figure S5). Mainly worm-like fibrillary structures in combination with long (> 200 nm) straight protein fibrils were observed after $OVA_{78/22h}$ and $EW_{100/15min}$ tryptic treatment (Figure 4 and Figure S4). In addition, the extract obtained after $OVA_{78/22h}$ tryptic treatment had characteristic amyloid green birefringence (Figure 4.s and Figure 4.f). Also, X-ray diffraction (Figure 4.u) showed meridional (4.7 Å) and equatorial (10.2 Å) reflections typical of intra-β-strand and inter-β-sheet distances of AFs, respectively. These results suggest that trypsin solubilised AFs from $OVA_{78/22h}$.



283

284 Figure 4. Characterisation of protein fibrils extracted with proteinase K and trypsin from heated
285 ovalbumin ($OVA_{78/22h}$) and egg white boiled for 15 min ($EW_{100/15min}$). TEM images $OVA_{78/22h}$ [(a)
286 to (i)] and $EW_{100/15min}$ [(j) to (r)] treated with proteinase K and trypsin over time. Scale bar: 200

nm. Congo red staining observed under bright (s) and cross-polar light (f) [Scale bar: 20 µm] and X-ray diffraction pattern (u) of $OVA_{78/22h}$ treated with trypsin.

As a control treatment, $OVA_{78/22h}$ was shaken in water for two days at 37 °C which resulted in decreased protein extractability (Figure 3.a) and increased ThT fluorescence (Figure 3.b). Also, the SE-HPLC profiles of $OVA_{78/22h}$ showed protein aggregates [elution time 9 – 12 min; molecular weight (MW) *ca.* 2,500 k; peak A] with higher ThT fluorescence when the samples had undergone this shaking treatment (Figure 3.c and Figure 3.d). In addition, long (> 200 nm) worm-like fibrillary aggregates were observed in peak A of shaken $OVA_{78/22h}$ samples (Figure S5). The observed increase in the level of fibrillary structures initially formed after heating OVA at 78 °C during further shaking at 37 °C (150 rpm, two days) is in line with earlier reports that mechanical agitation impacts the aggregation rate, size and morphology of protein fibrils[45,46]. When unheated OVA was shaken in water for two days at 37 °C protein aggregation also occurred but the ThT fluorescence remained low (data not shown). $EW_{100/15min}$ extracts contained about 10% protein (Figure 3.a) with apparent MWs < 74 k (elution time ≥ 18 min, Figure 3.e). Shaking of $EW_{100/15min}$ resulted in a negligible increase in the amount of peptides eluting between 17 and 18 min (MW *ca.* 74 k) in the SE-HPLC profiles and some ThT fluorescence enhancement (Figure 3.e and Figure 3.f).

Usage of chemicals for isolating protein fibrils

As an alternative for enzymatic extraction, chemicals were used to extract AF from $EW_{100/15min}$. Various concentrations of sodium dodecyl sulfate (SDS) and/or dithiothreitol (DTT) were used to impact non-covalent interactions and/or disulfide bonds, respectively. While SDS binds to proteins and modifies their secondary and tertiary structure[47,48], DTT reduces disulfide bridges in proteins into thiol groups. Mainly worm-like fibrillary structures of variable sizes were observed for

310 $EW_{100/15min}$ extracts in water and in 0.3% (w/v) SDS both in the presence (Figure S6) or absence
311 (Figure 6.j, Figure 6.k and Figure S6) of DTT. While all protein was extracted with 0.8% SDS
312 (w/v) containing DTT (Figure 5.c), such extraction resulted in lower (*ca*. 25%) ThT fluorescence
313 (Figure 5.d) than that with 0.3% SDS (w/v) containing DTT. TEM images (Figure 6.l and Figure
314 S6) of $EW_{100/15min}$ in 0.8% (w/v) SDS showed protein fibrils. However, while the FTIR spectra of
315 $EW_{100/15min}$ in 0.8% (w/v) SDS were characteristic for β-sheet structures, those in the same medium
316 also containing 1.0% (w/v) DTT were not (data not shown). With TEM, both amorphous
317 aggregates and protein fibrils were observed in the latter (Figure S6) The combined use of DTT
318 and the higher SDS concentrations for extracting protein from $EW_{100/15min}$ resulted in disruption of
319 protein fibrils.

320 The same chemical extractions procedures were applied on $OVA_{100/15min}$ samples as positive
321 control. While neither the protein extractability of unheated nor that of heated OVA were affected
322 by the concentrations of SDS and DTT used (Figure 5.a), the levels of ThT fluorescence were
323 (Figure 5.b). When using SDS concentrations in a 0.1% to 0.3% (w/v) range, the ThT fluorescence
324 of $OVA_{100/15min}$ samples increased from *ca.* 48% to *ca.* 85% irrespective of whether the medium
325 contained 1.0% (w/v) DTT (Figure 5.a). SDS thus also induced fibril formation in $OVA_{100/15min}$
326 samples. However, the ThT fluorescence of $OVA_{100/15min}$ samples was lower when the SDS levels
327 used exceeded 0.5% (w/v) both in the presence and absence of 1.0% (w/v) DTT (Figure 5.b). SDS
328 can thus also disrupt protein fibrils as also observed in unheated OVA samples at similar SDS
329 concentrations. In aqueous extracts of $OVA_{100/15min}$, mainly large (> 200 nm) intertwined worm-
330 like fibrillary aggregates were detected (Figure 6.d and Figure S6). At SDS concentrations of 0.3%
331 and 0.8% (w/v), the fibrils were *ca*. 100 nm (Figure 6.e and Figure S6) or *ca*. 40 nm (Figure 6.f
332 and Figure S6) long, respectively.

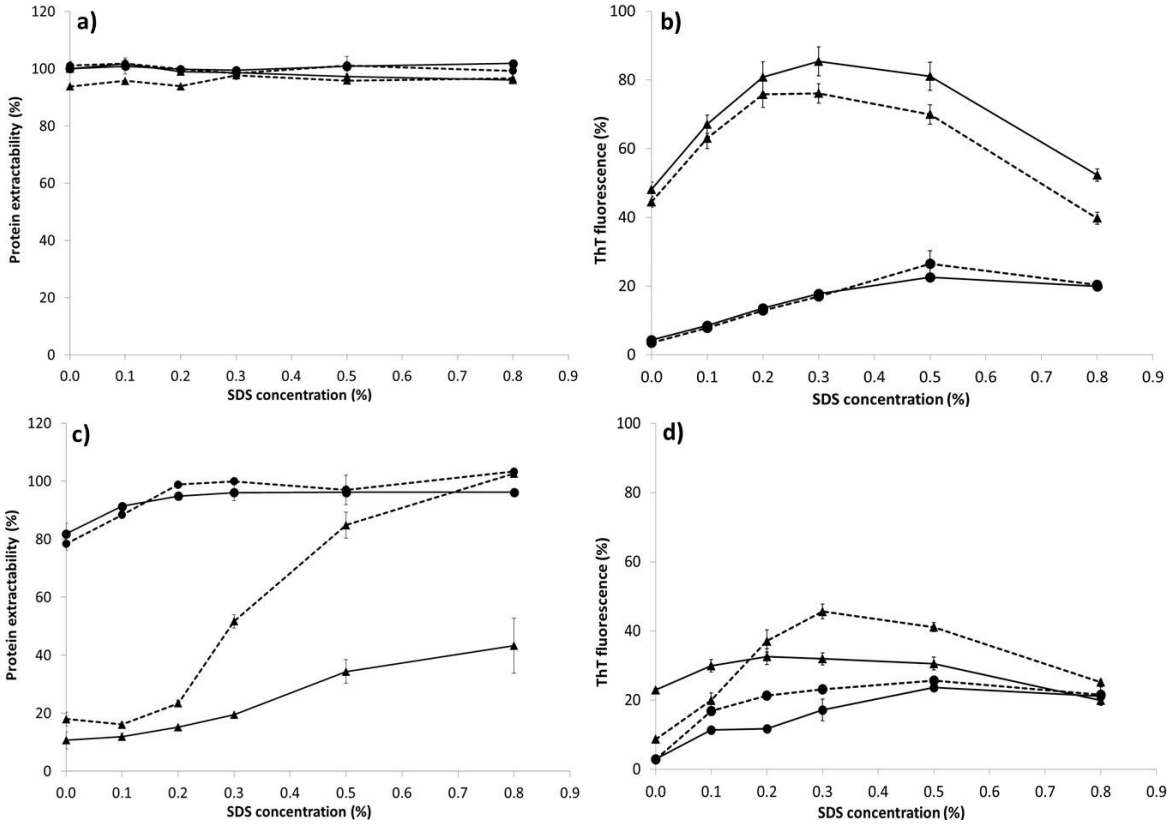


Figure 5. Impact of sodium dodecyl sulfate (SDS) and 1.0% (w/v) dithiothreitol (DTT) on protein fibril extractability from unheated ovalbumin (OVA) and egg white (EW) or boiled for 15 min OVA ($OVA_{100/15min}$) and EW ($EW_{100/15min}$). Protein extractability (a) and thioflavin T (ThT) fluorescence (b) of unheated OVA (a, b,●) and EW (c, d, ●) or $OVA_{100/15min}$ (a, b, ▲) and $EW_{100/15min}$ (c, d, ▲) extracted with various concentrations of SDS without (—) and with 1.0% (w/v) DTT (---).

To exclude that the chemical extraction procedure itself influenced the amyloid content of the sample, the procedure was performed under native conditions. Dilution (5x) and shaking (150 rpm) of fresh EW induced aggregation and precipitation of *ca*. 20% of the protein. Its extractability and ThT fluorescence gradually increased with SDS concentrations in the extraction medium (Figure

5.c and Figure 5.d). More EW protein was extractable when the SDS medium also contained DTT (Figure 5.c and Figure 5.d). Complete extractability was achieved with 0.8% (w/v) SDS irrespective of whether the medium also contained DTT (Figure 5.c). Mostly amorphous aggregates in combination with some large (> 200 nm) worm-like fibrillary structures were observed both in diluted EW (Figure 6.g and Figure S6) or in diluted EW containing 0.3% (w/v) SDS (Figure 6.h and Figure S6). Low concentrations of SDS may have induced the formation of fibrillary structures in EW but to a lesser extent than noted for OVA. TEM images of diluted EW in 1.0% (w/v) DTT showed mainly amorphous aggregates (Figure S6). In the case of diluted EW containing 0.3% (w/v) SDS and 0.8% (w/v) SDS along with DTT, TEM images indicated the presence of some worm-like fibrillary structures in combination with amorphous aggregates (Figure S6). The SDS induced fibril formation in diluted EW was thus enhanced by DTT.

Higher SDS concentrations [≥ 0.1% (w/v)] in solutions of unheated OVA lead to an increase in ThT fluorescence (Figure 5.b) from *ca.* 4% to *ca*. 20%, suggesting the formation of fibrillary structures. TEM images revealed that large (> 200 nm) intertwined worm-like fibrillary aggregates had been formed (Figure 6.a and Figure S6). OVA protein aggregates were smaller (< 200 nm) when resulting from bringing the protein in 0.3% (w/v) SDS (Figure 6.b and Figure S6) rather than in water. When brought in 0.8% (w/v) SDS, fibrillary aggregates of variable sizes were distinguished (Figure 6.c and Figure S6). Thus, SDS enhances fibrillation in solutions of unheated OVA. Presumably, SDS concentrations below its critical micellar concentration stabilize β-strands in unfolded proteins and thereby promote fibrillation. Micelles formed at high SDS concentrations limit fibril formation or disrupt fibrils already formed[47–50]. TEM images revealed worm-like fibrillary aggregates of various sizes in solutions of unheated OVA in water and in 0.3% (w/v) or 0.8% (w/v) SDS in combination with DTT (Figure S6). Reduction of the single intramolecular

disulfide bond in native OVA increases its surface hydrophobicity and may well facilitate protein fibrillation[29]. Overall, SDS concentrations up to 0.3% (w/v) either extracted fibrillary structures from or induced their formation in boiled OVA and EW, whereas SDS concentrations exceeding 0.5% (w/v) also disrupted fibrillary structures. These effects were enhanced when including 1.0% (w/v) DTT in SDS containing medium.

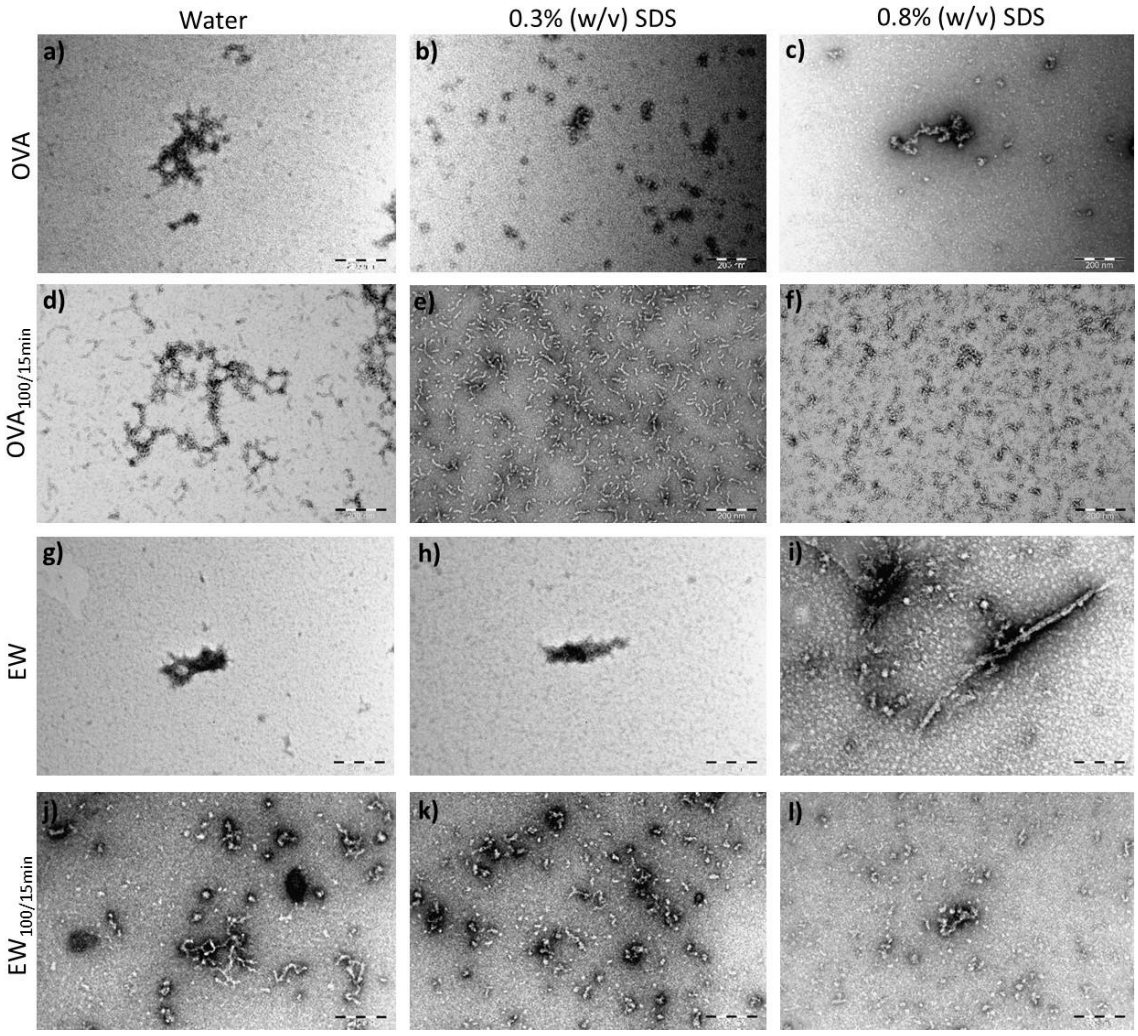


Figure 6. Morphology of fibrils of unheated ovalbumin (OVA) and egg white (EW) or boiled for 15 min OVA ($OVA_{100/15min}$) and EW ($EW_{100/15min}$) after isolation/extraction with sodium dodecyl sulfate (SDS). TEM images of unheated OVA and EW [(a) to (c) and (g) to (i), respectively] or

$OVA_{100/15min}$ [(d) to (f)] and $EW_{100/15min}$ [(j) to (l)] isolated/extracted with various concentrations of SDS. Scale bar: 200 nm.

CONCLUSIONS

Boiling EW leads to formation of AFs. EW fibrils were extracted with three different extraction procedures, suggesting the result is robust and independent of the extraction conditions. AF aggregation of proteins is driven by short aggregation-prone regions (APRs) within the protein sequence that form beta-structured assemblies while the rest of the protein chain decorates these clusters as unfolded polypeptides. In effect this creates a high local concentration of unfolded protein chains that is readily digestible by gastric proteases while only the APRs representing *ca.* 10% of the primary sequence remain protected. In comparison most of the proteolytic sites in a folded protein are not or much less accessible.

A dense worm-like fibrillary protein network is extracted from boiled EW with 0.01 M HCl from the pellet obtained after treating boiled EW with proteinase K. FTIR spectra, X-ray diffraction patterns and Congo red staining confirm the presence of AFs in this pellet. Treating heated OVA and boiled EW with trypsin extracts both amorphous and fibrillary aggregates while proteinase K mainly extracts amorphous structures. Prior treatment of heated OVA with trypsin allows elegant demonstration by X-ray diffraction and Congo red staining experiments that it contains AFs. Furthermore, SDS enhances the formation of fibrillary structures in both unheated and heated OVA and EW. Concentrations of SDS exceeding 0.5% (w/v) disrupt fibrillary protein structures, an effect which is enhanced in presence of DTT. Our results are the first to show that AFs are present in hard-boiled eggs. The presence of AFs in other food products should be explored. To study the latter, we suggest using an enzymatic extraction protocol as presented in this study. Also, the presence of AFs in hard-boiled egg white questions the role of AFs in the

400 human diet. It would be useful to study the proteolytic resistance of such protein structures in the
401 intestinal tract and to examine their toxicity. Such work will be the topic of a subsequent
402 manuscript. Last but not least, protein functionality can be optimised by exploiting AF formation.
403 Applications thereof include partial or total replacement of animal-based protein by plant proteins
404 in food systems.

405 *Supporting Information Available:* Morphology of (amyloid) protein fibrils in $EW_{100/15min}$ and
406 in unheated, heated and boiled OVA; Impact of peptidases on protein fibril extractability from
407 $OVA_{78/22h}$ and $EW_{100/15min}$ over time; Morphology of protein fibrils extracted with peptidases from
408 $OVA_{78/22h}$ and $EW_{100/15min}$; Morphology of the components in the SE-HPLC peaks in enzymatic
409 extracts of $OVA_{78/22h}$ and $EW_{100/15min}$; Morphology of protein fibrils of unheated OVA and EW or
410 $OVA_{100/15min}$ and $EW_{100/15min}$ isolated/extracted with SDS and 1.0% (w/v) DTT.

411 *Acknowledgments.* The authors acknowledge the Research Foundation-Flanders (FWO, SBO
412 grant S003918N Brussels, Belgium). M.A. Lambrecht acknowledges FWO-Flanders for her
413 mandate as postdoctoral researcher (grant 12V6718N). The Switch Laboratory was supported by
414 grants under the EU's Horizon 2020 Framework Programme ERC Grant agreement 647458
415 (MANGO) to J. Schymkowitz, the Flanders Institute for Biotechnology (VIB), the KU Leuven,
416 the FWO-Flanders, the Flanders Agency for Innovation by Science and Technology (IWT, SBO
417 grant 60839) and the Federal Office for Scientific Affairs of Belgium (Belspo), IUAP, grant
418 number P7/16. I. Rombouts and K.J.A. Jansens are gratefully thanked for fruitful discussions. L.
419 Liesenborghs and V. Depoortere are acknowledged for excellent technical assistance. The
420 Laboratory for biocrystallography (KU Leuven) and the Electron Microscopy Platform & Bio
421 Imaging Core (KU Leuven, VIB – KU Leuven Center for Brain & Disease Research) are gratefully
422 thanked for assistance with X-ray diffraction measurements and TEM analysis, respectively. M.

Monge-Morera thanks the University of Costa Rica (UCR) for the permission to perform research abroad. J.A. Delcour is W. K. Kellogg Chair in Cereal Science and Nutrition at the KU Leuven and beneficiary of Methusalem excellence funding at the KU Leuven.

REFERENCES

(1) Greenwald, J.; Riek, R. Biology of Amyloid: Structure, Function, and Regulation. *Structure* **2010**, *18*, 1244–1260.

(2) Serpell, L. Amyloid Structure. *Essays Biochem.* **2014**, *56*, 1–10.

(3) Knowles, T. P.; Fitzpatrick, A. W.; Meehan, S.; Mott, H. R.; Vendruscolo, M.; Dobson, C. M.; Welland, M. E. Role of Intermolecular Forces in Defining Material Properties of Protein Nanofibrils. *Sci. Reports* **2007**, *318*, 1900–1903.

(4) Knowles, T. P. J.; Mezzenga, R. Amyloid Fibrils as Building Blocks for Natural and Artificial Functional Materials. *Adv. Mater.* **2016**, *28*, 6546–6561.

(5) Pearce, F. G.; Mackintosh, S. H.; Gerrard, J. A. Formation of Amyloid-like Fibrils by Ovalbumin and Related Proteins under Conditions Relevant to Food Processing. *J. Agric. Food Chem.* **2007**, *55*, 318–322.

(6) Fowler, D. M.; Koulov, A. V.; Balch, W. E.; Kelly, J. W. Functional Amyloid - from Bacteria to Humans. *Trends Biochem. Sci.* **2007**, *32*, 217–224.

(7) Knowles, T. P. J.; Buehler, M. J. Nanomechanics of Functional and Pathological Amyloid Materials. *Nat. Nanotechnol.* **2011**, *6*, 469–479.

(8) Chiti, F.; Dobson, C. M. Protein Misfolding, Amyloid Formation, and Human Disease: A Summary of Progress over the Last Decade. *Annu. Rev. Biochem.* **2017**, *86*, 27–68.

(9) Rousseau, F.; Schymkowitz, J.; Serrano, L. Protein Aggregation and Amyloidosis: Confusion of the Kinds? *Curr. Opin. Struct. Biol.* **2006**, *16*, 118–126.

(10) Monsellier, E.; Ramazzotti, M.; Taddei, N.; Chiti, F. Aggregation Propensity of the Human Proteome. *PLoS Comput. Biol.* **2008**, *4*, e1000199.

(11) Eisenberg, D.; Jucker, M. The Amyloid State of Proteins in Human Diseases. *Cell* **2012**, *186*, 1188–1203.

(12) Knowles, T. P. J.; Vendruscolo, M.; Dobson, C. M. The Amyloid State and Its Association with Protein Misfolding Diseases. *Nat. Rev. Mol. Cell Biol.* **2014**, *15*, 384–396.

(13) Jansens, K. J. A.; Lambrecht, M. A.; Rombouts, I.; Monge Morera, M.; Brijs, K.; Rousseau, F.; Schymkowitz, J.; Delcour, J. A. Conditions Governing Food Protein Amyloid Fibril Formation—Part I: Egg and Cereal Proteins. *Compr. Rev. Food Sci. Food Saf.* **2019**, *0*, 1256–1276.

(14) Lambrecht, M. A.; Jansens, K. J. A.; Rombouts, I.; Brijs, K.; Rousseau, F.; Schymkowitz, J.; Delcour, J. A. Conditions Governing Food Protein Amyloid Fibril Formation—Part II: Milk and Legume Proteins. *Compr. Rev. Food Sci. Food Saf.* **2019**, *0*, 1277–1291.

(15) Solomon, A.; Richey, T.; Murphy, C. L.; Weiss, D. T.; Wall, J. S.; Westermark, G. T.; Westermark, P. Amyloidogenic Potential of Foie Gras. *PNAS* **2007**, *104*, 10998–11001.

(16) Mine, Y. Recent Advances in Egg Protein Functionality in the Food System. *Worlds. Poult. Sci. J.* **2002**, *58*, 31–39.

(17) Mine, Y.; Noutomi, T.; Hagu, N. Thermally Induced Changes in Egg White Proteins. *J. Agric. Food Chem.* **1990**, *38*, 2122–2125.

(18) Belitz, H.-D.; Grosch, W.; Schierberle, P. Eggs. In *Food Chemistry*; Springer: Berlin, Germany, 2009; pp 546–561.

(19) Weijers; van de Velde, F.; Stijnman, A.; van de Pijpekamp, A.; Visschers, R. W. Structure and Rheological Properties of Acid-Induced Egg White Protein Gels. *Food Hydrocoll.*

2006, *20*, 146–159.

(20) Astbury, W. T.; Dickinson, S.; Bailey, K. The X-Ray Interpretation of Denaturation and the Structure of the Seed Globulins. *Biochem. J.* **1935**, *29*, 2351–2360.

(21) Bhattacharya, M.; Dogra, P. Self-Assembly of Ovalbumin Amyloid Pores: Effects on Membrane Permeabilization, Dipole Potential, and Bilayer Fluidity. *Langmuir* **2015**, *31*, 8911–8922.

(22) Bhattacharya, M.; Jain, N.; Dogra, P.; Samai, S.; Mukhopadhyay, S. Nanoscopic Amyloid Pores Formed via Stepwise Protein Assembly. *J. Phys. Chem. Lett.* **2013**, *4*, 480–485.

(23) Jansens, K. J. A.; Brijs, K.; Stetefeld, J.; Delcour, J. A.; Scanlon, M. G. Ultrasonic Characterization of Amyloid-like Ovalbumin Aggregation. *ACS Omega* **2017**, *2*, 4612–4620.

(24) Lara, C.; Gourdin-Bertin, S.; Adamcik, J.; Bolisetty, S.; Mezzenga, R. Self-Assembly of Ovalbumin into Amyloid and Non-Amyloid Fibrils. *Biomacromolecules* **2012**, *13*, 4213–4221.

(25) Lassé, M.; Ulluwishewa, D.; Healy, J.; Thompson, D.; Miller, A.; Roy, N.; Chitcholtan, K.; Gerrard, J. A. Evaluation of Protease Resistance and Toxicity of Amyloid-like Food Fibrils from Whey, Soy, Kidney Bean, and Egg White. *Food Chem.* **2016**, *192*, 491–498.

(26) Weijers, M.; Sagis, L. M. C.; Veerman, C.; Sperber, B.; van der Linden, E. Rheology and Structure of Ovalbumin Gels at Low PH and Low Ionic Strength. *Food Hydrocoll.* **2002**, *16*, 269–276.

(27) Alting, A. C.; Weijers, M.; de Hoog, E. H. A.; van de Pijpekamp, A. M.; Cohen Stuart, M. A.; Hamer, R. J.; de Kruif, C. G.; Visschers, R. W. Acid-Induced Cold Gelation of Globular Proteins: Effects of Protein Aggregate Characteristics and Disulfide Bonding on

Rheological Properties. *J. Agric. Food Chem.* **2004**, *52*, 623–631.

(28) Azakami, H.; Mukai, A.; Kato, A. Role of Amyloid Type Cross β-Structure in the Formation of Soluble Aggregate and Gel in Heat-Induced Ovalbumin. *J. Agric. Food Chem.* **2005**, *53*, 1254–1257.

(29) Jansens, K. J. A.; Brijs, K.; Delcour, J. A.; Scanlon, M. G. Amyloid-like Aggregation of Ovalbumin: Effect of Disulfide Reduction and Other Egg White Proteins. *Food Hydrocoll.* **2016**, *61*, 914–922.

(30) Pouzot, M.; Nicolai, T.; Visschers, R. W.; Weijers, M. X-Ray and Light Scattering Study of the Structure of Large Protein Aggregates at Neutral PH. *Food Hydrocoll.* **2005**, *19*, 231–238.

(31) Tanaka, N.; Morimoto, Y.; Noguchi, Y.; Tada, T.; Waku, T.; Kunugi, S.; Morii, T.; Lee, Y. F.; Konno, T.; Takahashi, N. The Mechanism of Fibril Formation of a Non-Inhibitory Serpin Ovalbumin Revealed by the Identification of Amyloidogenic Core Regions. *J. Biol. Chem.* **2011**, *286*, 5884–5894.

(32) Weijers, M.; Barneveld, P. A.; Cohen Stuart, M. A.; Visschers, R. W. Heat-Induced Denaturation and Aggregation of Ovalbumin at Neutral PH Described by Irreversible First-Order Kinetics. *Protein Sci.* **2003**, *12*, 2693–2703.

(33) Weijers, M.; Visschers, R. W. Light Scattering Study of Heat-Induced Aggregation and Gelation of Ovalbumin. *Macromolecules* **2002**, *35*, 4753–4762.

(34) Numata, K.; Kaplan, D. L. Mechanisms of Enzymatic Degradation of Amyloid Beta Microfibrils Generating Nanofilaments and Nanospheres Related to Cytotoxicity. *Biochemistry* **2010**, *49*, 3254–3260.

(35) Hartl, F. U.; Bracher, A.; Hayer-Hartl, M. Molecular Chaperones in Protein Folding and

Proteostasis. *Nature* **2011**, *475*, 324–332.

(36) Harrison, R. S.; Sharpe, P. C.; Singh, Y.; Fairlie, D. P. Amyloid Peptides and Proteins in Review. In *Review of Physiology Biochemistry and Pharmacology*; Amara, S. G., Bamberg, E., Fleischmann, B., Gudermann, T., Hebert, S. C., Jahn, R., Lederer, W. J., Lilll, R., Hiyajima, A., Offermanns, S., Zechner, R., Eds.; Springer, Berlin, 2007; Vol. 159, pp 1–77.

(37) Maurer-Stroh, S.; Debulpaep, M.; Kuemmerer, N.; Lopez de la Paz, M.; Martins, I. C.; Reumers, J.; Morris, K. L.; Copland, A.; Serpell, L. C.; Serrano, L.; Schymkowitz, J. W. H.; Rousseau, F. Exploring the Sequence Determinants of Amyloid Structure Using Position-Specific Scoring Matrices. *Nat. Methods* **2010**, *7*, 237–242.

(38) Vassar, P. S.; Culling, C. F. Fluorescent Stains, with Special Reference to Amyloid and Connective Tissues. *Arch. Pathol.* **1959**, *68*, 487–498.

(39) Stsiapura, V. I.; Maskevich, A. A.; Kuzmitsky, V. A.; Uversky, V. N.; Kuznetsova, I. M.; Turoverov, K. K. Thioflavin T as a Molecular Rotor: Fluorescent Properties of Thioflavin T in Solvents with Different Viscosity. *J. Phys. Chem. B* **2008**, *112*, 15893–15902.

(40) Hackl, E. V.; Darkwah, J.; Smith, G.; Ermolina, I. Effect of Acidic and Basic PH on Thioflavin T Absorbance and Fluorescence. *Eur. Biophys. J.* **2015**, *44*, 249–261.

(41) Randrianjatovo-Gbalou, I.; Marcato-Romain, C. E.; Girbal-Neuhauser, E. Quantification of Amyloid Fibrils Using Size Exclusion Chromatography Coupled with Online Fluorescence and Ultraviolet Detection. *Anal. Biochem.* **2015**, *488*, 19–21.

(42) Nichols, M. R.; Moss, M. A.; Reed, D. K.; Lin, W. L.; Mukhopadhyay, R.; Hoh, J. H.; Rosenberry, T. L. Growth of β-Amyloid(1-40) Protofibrils by Monomer Elongation and Lateral Association. Characterization of Distinct Products by Light Scattering and Atomic Force Microscopy. *Biochemistry* **2002**, *41*, 6115–6127.

(43) Leslie, A. G. W.; Powell, H. R. Processing Diffraction Data with Mosflm. In *Evolving Methods for Macromolecular Crystallography*; Read, R. J., Sussman, J. L., Eds.; Springer: Dordrecht, The Netherlands, 2007; Vol. 245, pp 41–51.

(44) Nilsson, M. R. Techniques to Study Amyloid Fibril Formation in Vitro. *Methods* **2004**, *34*, 151–160.

(45) Sivalingam, V.; Prasanna, N. L.; Sharma, N.; Prasad, A.; Patel, B. K. Wild-Type Hen Egg White Lysozyme Aggregation in Vitro Can Form Self-Seeding Amyloid Conformational Variants. *Biophys. Chem.* **2016**, *219*, 28–37.

(46) Petkova, A. T.; Leapman, R. D.; Guo, Z.; Yau, W.-M.; Mattson, M. P.; Tycko, R. Self-Propagating, Molecular-Level Polymorphism in Alzheimer's β-Amyloid Fibrils. *Science* **2005**, *307*, 262–266.

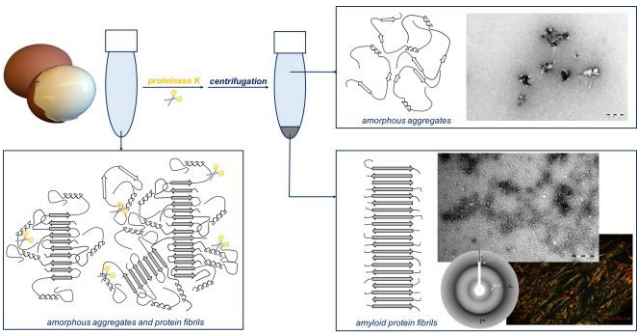
(47) Pertinhez, T. A.; Bouchard, M.; Smith, R. A. G.; Dobson, C. M.; Smith, L. J. Stimulation and Inhibition of Fibril Formation by a Peptide in the Presence of Different Concentrations of SDS. *FEBS Lett.* **2002**, *529*, 193–197.

(48) Yamamoto, S.; Hasegawa, K.; Yamaguchi, I.; Tsutsumi, S.; Kardos, J.; Goto, Y.; Gejyo, F.; Naiki, H. Low Concentrations of Sodium Dodecyl Sulfate Induce the Extension of Beta 2-Microglobulin-Related Amyloid Fibrils at a Neutral PH. *Biochemistry* **2004**, *43*, 11075–11082.

(49) Yagi, H.; Ban, T.; Morigaki, K.; Naiki, H.; Goto, Y. Visualization and Classification of Amyloid Supramolecular Assemblies. *Biochemistry* **2007**, *46*, 15009–15017.

(50) Rangachari, V.; Reed, D. K.; Moore, B. D.; Rosenberry, T. L. Secondary Structure and Interfacial Aggregation of Amyloid-Beta(1-40) on Sodium Dodecyl Sulfate Micelles. *Biochemistry* **2006**, *45*, 8639–8648.

561 TABLE OF CONTENTS GRAPHIC

562 

563

564

565